Water Management
Volume 164 Issue WM10

Anthropogenic impact assessment of Niangziguan karst water
Gao, Wang, Ma, *et al.*

ice | proceedings

Proceedings of the Institution of Civil Engineers
Water Management 164 November 2011 Issue WM10
Pages 495–510 http://dx.doi.org/10.1680/wama.1000070
Paper 1000070
Received 11/07/2010 Accepted 08/12/2010
Published online 12/09/2011
Keywords: groundwater/pollution/water supply

ice Institution of Civil Engineers publishing

Anthropogenic impact assessment of Niangziguan karst water

1 **Xubo Gao** PhD
Post-doctoral Fellowship, MOE Key Laboratory of Biogeology and Environmental Geology and School of Environmental Studies, China University of Geosciences, Wuhan, PR China

2 **Yanxin Wang** PhD
Professor, MOE Key Laboratory of Biogeology and Environmental Geology and School of Environmental Studies, China University of Geosciences, Wuhan, PR China

3 **Teng Ma** PhD
Professor, MOE Key Laboratory of Biogeology and Environmental Geology and School of Environmental Studies, China University of Geosciences, Wuhan, PR China

4 **Qinhong (Max) Hu** PhD
Assistant Professor, Department of Earth and Environmental Sciences, University of Texas at Arlington, USA

5 **Xingli Xing** PhD
Post-doctoral Fellowship, MOE Key Laboratory of Biogeology and Environmental Geology and School of Environmental Studies, China University of Geosciences, Wuhan PR China

6 **Qian Yu**
MSc Student, MOE Key Laboratory of Biogeology and Environmental Geology and School of Environmental Studies, China University of Geosciences, PR China






As the biggest karst spring system in northern China, the Niangziguan karst water system is the major source of water supply for Yangquan city, one of the most important bases of coal production in China. In this study, the chemical composition of karst groundwater was investigated with particular emphasis on identifying the sources of chemical variation. The results show significant geographic variation in chemical constituents through the karst groundwater system and also indicate that human activity is responsible for much of the observed hydrochemical variation. The addition of SO_4^{2-}, Cl^- and NO_3^- from human activities causes the groundwater hydrochemistry to vary from the HCO_3-Ca-Mg or HCO_3-SO_4-Ca-Mg type to the SO_4-HCO_3-Ca, Cl-SO_4-HCO_3-Ca, SO_4-Ca or SO_4-Cl-Ca type. Results from factor analysis indicate that abnormally high levels of SO_4^{2-} and Na^+ are from sources related to coal mining activity, which is widely distributed in the study area. High concentrations of Cl^- and NO_3^- result from sources related to human activities such as agriculture and mining wastewaters and sewage discharge. The results of cluster analysis in combination with hydrogeochemical analysis indicate that natural and anthropogenic processes jointly control the evolution of groundwater chemistry in regional groundwater systems like Niangziguan.

1. Introduction

As the source of water supply for about 25% of the global population (Ford and Williams, 2007), studying karst groundwater is critical for sustainable development of human society. In northern China, over 50% of the drinking water supply derives from karst aquifers and in some regions karst groundwater is the only available source of fresh water. Karst aquifers have complex and distinct characteristics that make them very different from other types of aquifers (Bakalowicz, 2005). Karst aquifers tend to have a high vulnerability to input of contaminants because of possibly thin soil layers, numerous sinkholes and other direct contaminant pathways. Over recent years, karst water systems have been under increasing risk of contamination due to population growth and industrial and agricultural activities.

Within a karst system, there are both extremely fast and

extremely slow flow components, and contaminants can be either transported very rapidly or held in storage for a long time. The highly interconnected fissures in a karst system can make pollution spread quickly and widely (Baker and Groves, 2008; Bonacci *et al.*, 2009; LeGrand, 1984). Urban runoff, wastewater discharge and solid waste disposal have added organic and inorganic pollutants such as nitrogen, phosphate, chloride, sulphate and heavy metals into groundwater systems (Gao *et al.*, 2007; Glassmeyer *et al.*, 2005; Jackson *et al.*, 2001). Coal mining activity and fertiliser application have significantly elevated the concentrations of sulphate and nitrate in groundwater (Aravena *et al.*, 1999; Denimal *et al.*, 2002; Ghiglieri *et al.*, 2009; Moncaster *et al.*, 2000; Spalding and Exner, 1993; Williams *et al.*, 2001; Zhang *et al.*, 1996). In China, especially northern China, groundwater pollution in karst areas has recently gained special attention (Gao *et al.*, 2010; Hatano *et al.*, 2002; Jiang *et al.*, 2009; Wang *et al.*, 2001; Yuan, 1997).

As a major diagnostic tool in groundwater hydrology, hydrogeochemical data collection, coupled with multi-dimensional data analysis, has been used to understand specific hydrogeochemical processes (Helena *et al.*, 2000; Reghunath *et al.*, 2002; Thyne *et al.*, 2004; Wang *et al.*, 2001). Multi-variate statistical techniques have been used to reduce the number of variables or cases while in principle retaining the same information as in the original data. Factor and cluster analyses, which are among the most widely used multi-variate statistical techniques, have been successfully applied to clarify the contributing hydrogeochemical processes controlling groundwater quality and to identify pollution sources in groundwater systems (Farnham *et al.*, 2000; Glynn and Plummer, 2005; Reghunath *et al.*, 2002; Silliman *et al.*, 2007).

In the present study, statistical models were employed and combined with hydrogeochemical analysis to further understand the impacts of human activity on the groundwater hydrochemistry of the Niangziguan carbonate area (referred to here as the Niangziguan karst water system (NKWS)) in northern China.

2. Geological and hydrogeological setting of the NKWS

The NKWS contains three lithostratigraphic units (Figures 1 and 2):

(*a*) Archaean metamorphic rocks
(*b*) Paleozoic carbonate, sandstone and shale
(*c*) Cenozoic alluvium (clay, sand and gravel).

The Paleozoic carbonate formation constitutes the main aquifers, and can be divided into four parts. The lowest part is the Cambrian formation that consists of limestone, dolomitic limestone and dolomite with a total thickness of 120 m. The next lowest Paleozoic unit consists of shale and mudstone that function as the regional basal aquitard of the karst water system. The middle part of the system consists of Ordovician limestone and dolomite, which form the two main aquifers. The limestone aquifer overlies the dolomite and is composed of calcite with three interlayers of gypsum; the thickness of limestone ranges up to 300–600 m and that of dolomite 120–180 m in southern and western areas of recharge. There are many karst fractures, karst caves and conduits in the middle section. The upper part of the system is made up of Carboniferous–Permian coal-bearing formations that consist of limestone, shale and coal.

The northern, western and southern boundaries of the study area are high in topography; the lowest point of the area is located in the east, in Niangziguan town, where springs emerge. Historically, groundwater was recharged primarily in the high elevations around the perimeter of the study area and was discharged primarily through springs and human usage. During recent years, over-exploitation of the karst groundwater has led to a serious decline of the water table in the study area (Hao *et al.*, 2009; Wang and Gao, 2009). Cones of depression have been formed in the areas of Yangquan, Pingdin and Shouyang counties (Figure 1) and local recharge of groundwater in these areas may become important. In this study, NKWS is divided into the following subareas: the original recharge area, the flow-through area and the discharge areas (Figure 3).

3. Sampling and method

Samples were collected between November 2006 and September 2009. These included ten surface water samples, 25 karst water samples, five spring water samples, four mining wastewater samples and three fissured rock water samples. The general characteristics of the collected samples and sampling sites are given in Table 1. The locations of the sampling sites were determined using a portable global positioning system. When sampling, all water samples were filtered on site through 0·45 μm membranes. Each water sample was divided among four 550 ml polyethylene bottles. For cation analyses, reagent-quality HNO_3 was added to one of the bottles until the pH of the sample reached 1. Before sampling, the bottles had been rinsed with deionised water and twice with the sample water. Field parameters, including water temperature, pH and electrical conductivity (EC), were measured in situ using portable Hanna EC and pH meters that had been calibrated before use. Alkalinity was measured on the sampling day using the Gran titration method. Concentrations of anions in the samples were determined using ion chromatography (Dionex 120) and the cation contents were analysed using ICP-AES (inductive coupled plasma emission spectrometry, Thermo Fisher Scientific), following US Environmental Protection Agency standard methods. The estimated analytical errors were within 5% (Table 2). The $^{18}O/^{16}O$ ratio of natural water was determined using the common CO_2–H_2O equilibration technique in which millimole (mmol) quantities of CO_2 were equilibrated with 5 ml of the water sample under constant temperature and shaken gently for 18 h (Epstein and Mayeda, 1953). Subsequently, the CO_2 was cryogenically purified and analysed by a dual-inlet isotope ratio mass spectrometer for its $^{18}O/^{16}O$ ratio. The obtained 'raw' $\delta^{18}O$–H_2O values were drift-corrected and normalised using internal laboratory standards. Corrected $\delta^{18}O$–H_2O values are reported in mil (‰)

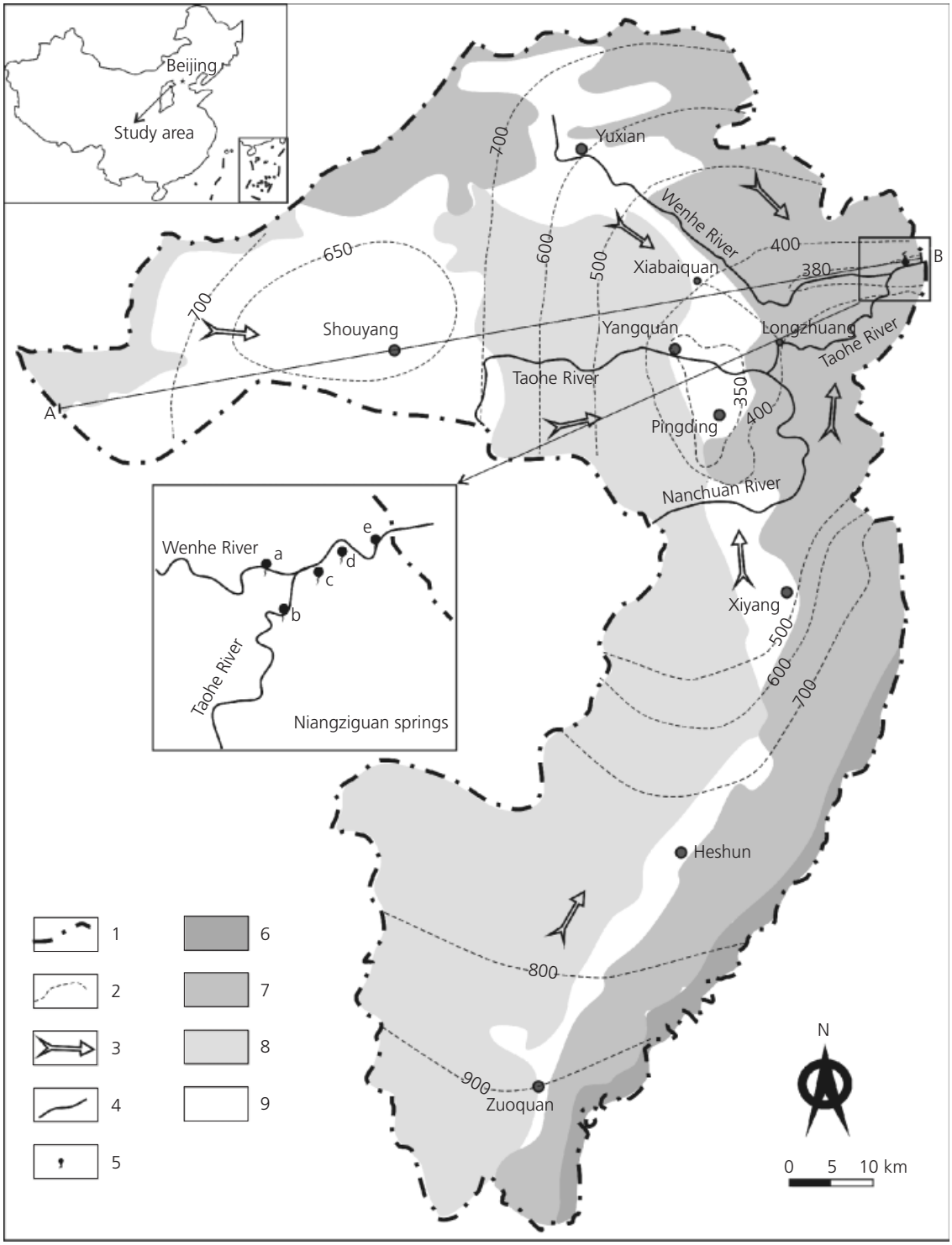

Figure 1. A simple hydrogeological map of NKWS. 1, the boundary of the study area; 2, groundwater counter line; 3, groundwater flow direction; 4, river; 5, spring; 6; Archaean; 7, Middle Ordovician limestone; 8, carboniferous Permian formation; 9, Quaternary. Niangziguan springs: a, Podi spring; b, Chenxi spring; c, Wulong spring; d, Shuiliandong spring; e, Weizeguan spring. A–B: geological cross-section

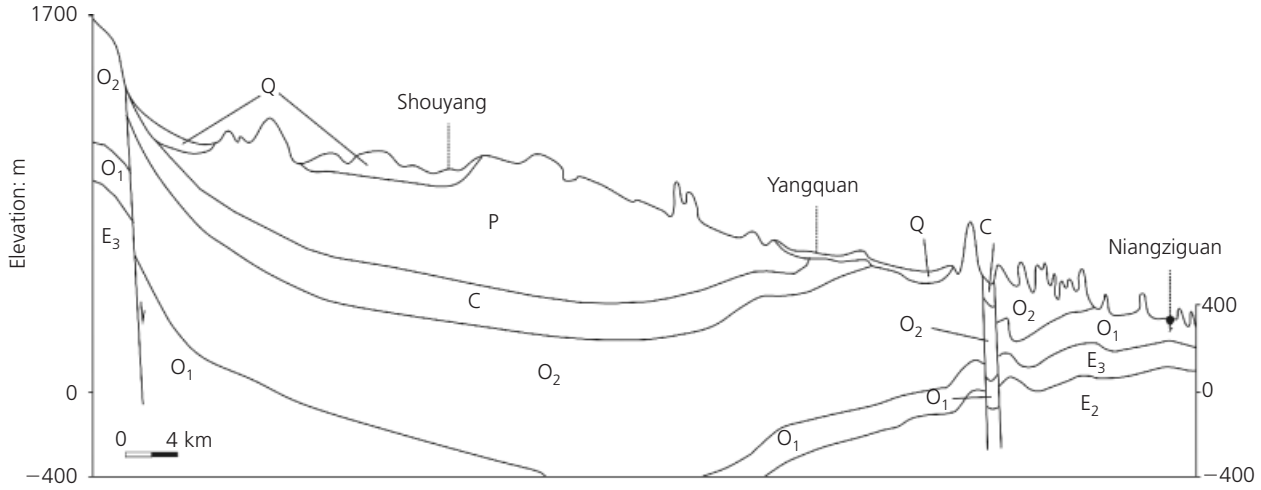

Figure 2. The A–B geological cross-section in the study area (see Figure 1). Q, Cenozoic alluvium; P, Permian sandstone and shale; C, Carboniferous sandstone and shale; O_1, lower Ordovician carbonates; O_2, middle Ordovician carbonates; E_2, middle Cambrian carbonates; E_3, upper Cambrian carbonates

notation relative to Vienna standard mean ocean water (V-SMOW).

Statistical techniques, including box and whisker plot and factor and cluster analyses of the water hydrochemistry data, were performed using Statistica software version 9·0. Factor analysis of the hydrochemistry data was used to assess the contributions of anthropogenic processes to the hydrochemistry of karst water in the NKWS. Factor extraction was carried out by principal component analysis. Varimax rotation was applied to obtain uncorrelated components. Clusters were calculated using the factor scores of water samples by means of *k*-means clustering, which attempts to find the centres of natural clusters in data.

4. Results and discussion

4.1 Hydrochemistry

Several chemically different groundwater types were recognised at NKWS (Table 1). The groundwater is normally slightly alkaline to alkaline (pH 7·12–8·05) with a temperature of 16·8–20·0°C. Most of the groundwater samples (nos 2, 27, 24, 47) collected from the recharge areas were HCO_3-Ca-Mg or HCO_3-SO_4-Ca-Mg type waters, characterised by low water temperature (less than 19·0°C) and slightly alkaline to alkaline (pH 7·27–7·98). Groundwater samples collected from flow-through areas included HCO_3, HCO_3-SO_4, HCO_3-Cl/SO_4-HCO_3, SO_4, SO_4-Cl-HCO_3 and Cl-SO_4-HCO_3 type waters with Ca^{2+} and Mg^{2+} as the dominant cations.

The karst springs were generally SO_4-Ca-Mg or SO_4-HCO3-Ca-Mg type waters, with temperatures between 18·0 and 20·0°C and pH of 7·36–8·40.

Surface water samples almost all belonged to SO_4 type water, including SO_4, SO_4-HCO_3 and SO_4-Cl types, with Ca^{2+} as the dominant cation. The only HCO_3-SO_4-Ca type surface water was collected from the headwater of the Taohe River where the surface water was recharged by mountain streams. The surface waters were also slightly alkaline to alkaline (pH 7·48–10·12; average 8·29) with a temperature of 22·0–30·0°C.

Mining wastewaters, collected from four representative coal mines, were all SO_4-Ca-Mg or SO_4-Ca type and showed the highest sulphate contents (1028–4217 mg/l) and low bicarbonate contents (less than 160 mg/l). They were slightly acidic to acidic (pH 3·80–6·50) and saline (total dissolved solids (TDS) from 1·69 to 5·86 g/l), with temperatures of 18·5–23·5°C. Discharge or leakage of mining wastewater into the surface water or groundwater may therefore cause a dramatic elevation in sulphate content and TDS.

Groundwater from the recharge area showed stable isotope composition, from −9·93 to −6·80‰ for $\delta^{18}O$ and −69·0 to −50·2‰ for δD (Table 2). Owing to evaporation effects, most surface water samples had elevated $\delta^{18}O$ values and the δD values decreased in the following order: surface water, mining wastewater, karst water from the flow-through area, water in fissured rocks, karst water from the recharge area and karst spring water. Along the flow path (Figure 4), relatively high $\delta^{18}O$ and δD values were also found in some groundwater samples from mining areas, industrial and densely populated residential areas and the flow-through area (Figure 3), indicating the impact of coal mining and municipal wastewater discharge on karst water.

A summary of the descriptive statistics for physico-chemical

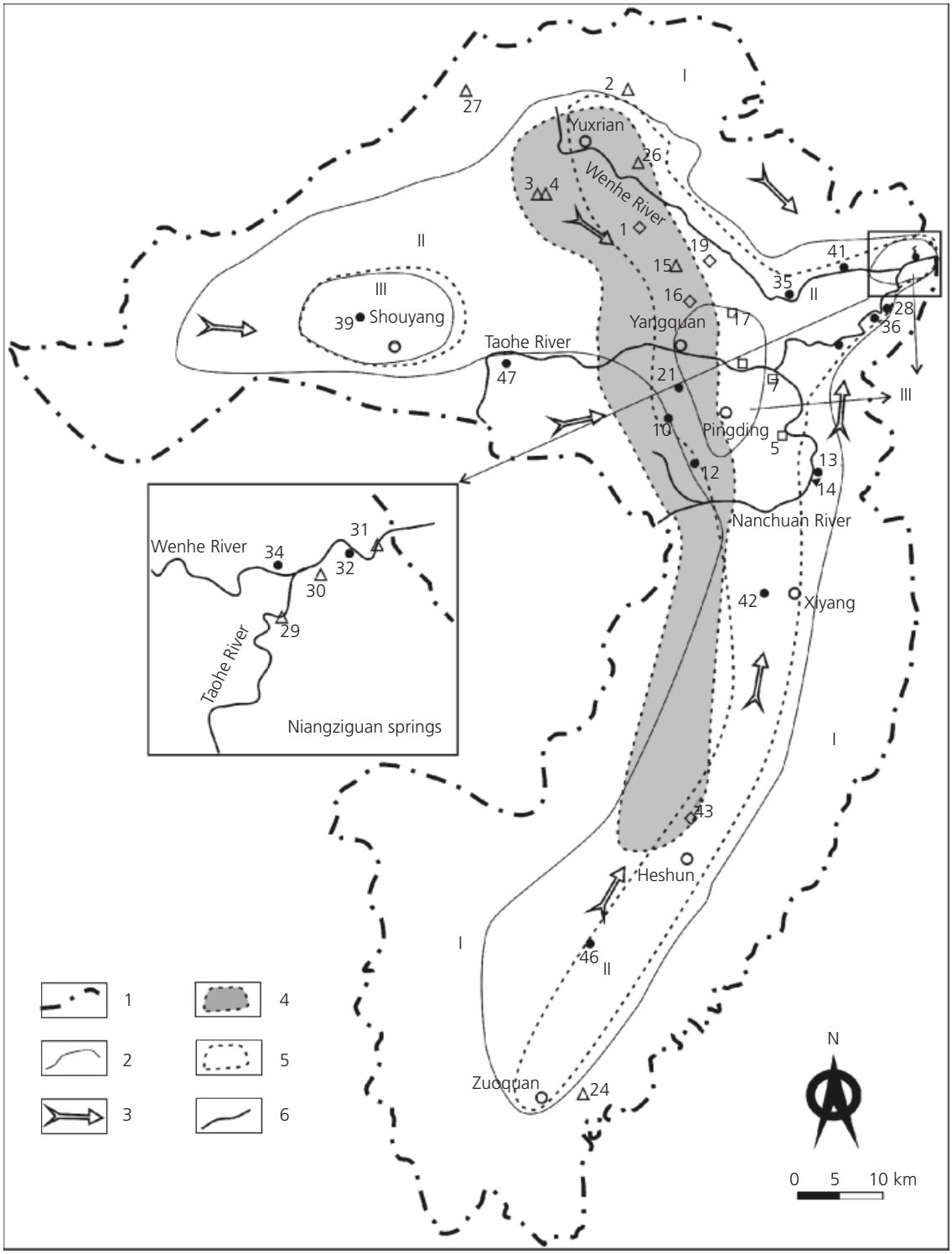

Figure 3. Distribution of groundwater (including spring waters) with different factor scores. 1, boundary of the study area; 2, boundary of the subareas (I, recharge area; II, flow-through area; III, discharge area (natural and artificial discharge)); 3, groundwater flow direction; 4, coal mining area; 5, industrial areas and densely populated residential areas; 6, river. Samples cluster: ◇, cluster 1; □, cluster 2; ●, cluster 3; △, cluster 4

Sample no.	Type of sample*	Latitude	Longitude	Age of aquifer	Depth: m	Water type
1	KW	113°28′39·1″	38°02′12·4″	Middle Ordovician	700·0	SO_4-HCO_3-Ca-Mg
2	KW	113°27′53·0″	38°06′07·8″	Middle Ordovician	650·0	HCO_3-Ca-Mg
3	FW	113°23′01·7″	38°02′42·4″	Permian	200·0	HCO_3-SO_4-Ca-Mg
4	KW	113°23′01·7″	38°02′42·4″	Middle Ordovician	600·0	SO_4-HCO_3-Ca-Mg
5	KW	113°42′2·9″	37°47′13·6″	Middle Ordovician	400·0	SO_4-Cl-HCO_3-Ca-Mg
6	SW	113°42′13·4″	37°47′21·7″	—	—	SO_4-HCO_3-Ca-Mg
7	KW	113°41′42·9″	37°50′44·6″	Middle Ordovician	400·0	HCO_3-Cl-Ca
8	SW	113°41′29·2″	37°50′56·2″	—	—	SO_4-HCO_3-Ca-Na-Mg
9	SW	113°47′58·1″	37°53′49·6″	—	—	SO_4-Cl-Ca-Na-Mg
10	KW	113°34′40·3″	37°48′20·2″	Middle Ordovician	500·0	SO_4-HCO_3-Cl-Ca
11	SW	113°31′38·0″	37°46′21·7″	—	—	SO_4-HCO_3-Ca-Mg
12	KW	113°33′57·6″	37°45′41·6″	Middle Ordovician	650·0	HCO_3-SO_4-Ca
13	KW	113°44′38·2″	37°44′49·8″	Middle Ordovician	600·0	SO_4-HCO_3-Ca-Mg
14	SW	113°33′20·4″	37°58′59·9″	—	—	SO_4-Ca
15	KW	113°33′20·5″	37°58′59·9″	Middle Ordovician	500·0	SO_4-HCO_3-Ca-Mg
16	KW	113°34′37·1″	37°57′41·2″	Middle Ordovician	500·0	SO_4-Ca-Mg
17	KW	113°36′42·7″	37°53′17·8″	Middle Ordovician	630·0	Cl-SO_4-HCO_3-Ca-Mg
18	KW	113°38′30·9″	37°50′29·7″	Middle Ordovician	700·0	SO_4-HCO_3-Ca-Mg
19	KW	113°38′0·1″	37°54′47·7″	Middle Ordovician	739·0	SO_4-HCO_3-Ca-Mg
20	MW	113°33′20·6″	37°58′59·8″	—	612·0	SO_4-Ca-Mg
21	FW	113°32′22·6″	37°49′53·0″	Carboniferous	5·0	HCO_3-SO_4-Ca
22	MW	113°31′12·8″	37°52′14·4″	—	—	SO_4-Ca
23	MW	113°30′43·8″	37°54′44·2″	—	—	SO_4-Ca-Mg
24	KW	113°21′30·8″	37°03′34·8″	Middle Ordovician	500·0	HCO_3-SO_4-Ca-Mg
25	SW	113°36′32·1″	37°51′10·2″	—	—	SO_4-Cl-Ca-Na-Mg
26	KW	113°28′26·5″	38°03′55·0″	Lower Ordovician	680·0	HCO_3-Ca-Mg
27	KW	113°19′32·2″	38°13′11·8″	Middle Ordovician	—	HCO_3-Ca-Mg
28	KW	113°50′46·3″	37°55′23·5″	Middle Ordovician	80·0	SO_4-HCO_3-Cl-Ca-Na-Mg
29	SP	113°51′26·2″	37°57′06·8″	—	—	HCO_3-SO_4-Ca-Mg
30	SP	113°52′27·6″	37°57′47·0″	—	—	HCO_3-SO_4-Ca-Mg
31	SP	113°53′28·6″	37°57′58·8″	—	—	HCO_3-SO_4-Ca-Mg
32	SP	113°52′59·0″	37°58′08·8″	—	—	SO_4-HCO_3-Ca-Mg
33	SW	113°52′58·1″	37°58′10·4″	—	—	SO_4-HCO_3-Ca-Mg
34	SP	113°50′59·4″	37°57′47·7″	—	—	SO_4-HCO_3-Ca-Mg
35	KW	113°43′14·5″	37°56′25·4″	Middle Ordovician	350·8	SO_4-HCO_3-Ca-Mg
36	KW	113°46′45·0″	37°52′58·6″	Middle Ordovician	140·0	SO_4-HCO_3-Cl-Ca-Mg
37	SW	113°32′42·9″	38°02′14·4″	—	—	SO_4-Ca-Mg
38	MW	113°32′32·9″	37°51′28·0″	—	Discharged	SO_4-Ca-Mg
39	KW	113°31′52·7″	37°51′09·5″	Middle Ordovician	457·0	SO_4-Ca-Mg
40	KW	113°43′54·2″	37°51′59·2″	Middle Ordovician	201·7	HCO_3-Ca-Mg
41	KW	113°49′14·6″	37°57′25·4″	Middle Ordovician	150·9	SO_4-Ca-Mg
42	KW	113°39′05·3″	37°37′17·2″	Middle Ordovician	610·0	HCO_3-SO_4-Ca
43	KW	113°32′37·6″	37°24′53·8″	Middle Ordovician	820·0	SO_4-HCO_3-Ca-Mg
44	SW	113°28′26·5″	38°03′55·0″	—	—	SO_4-HCO_3-Ca
45	SW	113°23′02·4″	37°52′22·9″	—	—	HCO_3-SO_4-Ca
46	KW	113°27′06·3″	37°15′12·4″	Middle Ordovician	600·0	SO_4-HCO_3-Ca
47	FW	113°22′41·5″	37°51′58·3″	Carboniferous	2·0	HCO_3-SO_4-Ca-Mg

* KW, karst water; FW, groundwater in fissured rocks; SW, surface water; MW, mining wastewater; SP, spring water

Table 1. Sampling locations and water types

Sample no.	*T*: °C	pH	EC: μS/cm	Ion concentration: mg/l								$\delta^{18}O$: ‰	δD: ‰	TDS: g/l
				K^+	Na^+	Ca^{2+}	Mg^{2+}	Cl^-	SO_4^{2-}	HCO_3^-	NO_3^-			
1	19·5	7·12	1693	0·44	31·90	280·0	72·9	28·4	750·0	284·0	25·3	−8·55	−61·8	1·47
2	18·0	7·46	461	0·01	4·49	63·1	20·1	9·9	10·2	265·0	13·7	−9·93	−69·0	0·39
3	18·0	7·32	762	0·01	17·70	100·0	30·6	32·6	132·0	272·0	16·1	−8·98	−65·8	0·60
4	19·0	7·27	959	0·02	10·20	137·0	49·6	17·7	257·0	311·0	28·8	−9·45	−66·4	0·81
5	20·0	7·23	1703	2·28	69·80	227·0	47·6	141·0	386·0	240·0	149·0	−7·24	−54·1	1·26
6	28·0	7·81	2470	11·70	122·00	331·0	72·8	18·6	976·0	388·0	77·4	−6·39	−59·1	2·00
7	20·0	7·33	1584	2·45	58·10	215·0	42·4	154·0	68·3	539·0	143·0	−7·98	−55·8	1·22
8	29·0	7·48	1725	9·61	137·00	154·0	46·7	76·6	489·0	237·0	107·0	−8·00	−57·6	1·26
9	30·0	10·12	1489	6·94	131·00	117·0	40·7	144·0	470·0	23·1	69·5	−6·91	−52·6	1·00
10	18·0	7·65	1068	0·14	37·40	198·0	32·8	146·0	249·0	274·0	30·3	−8·35	−57·2	0·97
11	22·0	7·50	722	0·01	9·49	94·3	33·8	19·7	229·0	129·0	30·4	−8·89	−63·0	0·55
12	18·0	7·98	479	0·27	10·60	67·4	11·5	15·6	81·2	145·0	15·4	−6·85	−50·2	0·35
13	20·0	7·50	880	0·28	9·20	139·0	30·4	18·4	241·0	215·0	51·7	−8·35	−61·7	0·70
14	22·0	7·90	1230	3·93	19·00	219·0	30·6	31·9	574·0	61·6	43·7	−6·74	−54·4	0·98
15	18·2	7·53	1033	0·16	14·20	156·0	46·0	21·3	63·3	582·0	49·5	−9·42	−66·3	0·93
16	17·3	7·37	1637	1·51	51·10	244·0	67·3	53·5	638·0	256·0	6·5	−9·39	−64·2	1·32
17	18·6	7·86	1320	0·31	69·90	121·0	44·3	244·0	52·6	209·0	85·1	−8·56	−61·8	0·83
18	16·8	7·70	957	0·92	35·10	122·0	31·2	63·7	153·0	250·0	68·5	−8·52	−61·4	0·72
19	18·5	7·68	1805	0·73	22·30	258·0	74·7	24·4	687·0	320·0	17·6	−8·83	−61·9	1·41
20	18·5	5·07	4293	7·31	196·00	432·0	124·0	76·5	2243·0	5·5	2·2	−8·15	−57·6	3·09
21	15·5	7·71	550	0·02	8·18	84·3	14·7	16·4	77·1	166·0	63·0	−8·75	−61·3	0·43
22	22·0	5·16	4090	5·92	194·00	182·0	65·7	10·8	1346·0	4·8	2·4	−9·25	−65·2	1·81
23	22·0	3·80	4670	3·88	857·00	411·0	362·0	12·4	4217·0	0·0	3·5	−8·48	−59·8	5·87
24	18·2	7·68	480	1·50	8·18	54·2	19·2	10·6	80·4	204·0	9·2	−9·08	−63·4	0·39
25	26·5	8·25	1500	2·60	116·00	205·0	35·5	182·0	487·0	159·0	4·5	−7·48	−60·7	1·19
26	19·0	7·53	634	0·02	6·19	75·1	23·6	11·9	48·4	256·0	28·1	−9·55	−69·0	0·45
27	15·7	7·53	563	0·02	3·49	73·0	26·1	6·13	26·3	324·0	13·3	−9·69	−66·7	0·47
28	18·0	7·48	1653	3·99	98·30	180·0	49·1	154·0	307·0	308·0	110·0	−7·86	−57·8	1·21
29	18·0	7·52	851	0·76	29·50	99·4	31·0	54·6	96·1	262·0	60·0	−9·14	−66·3	0·63
30	19·0	7·50	926	0·55	33·40	108·0	34·8	64·5	108·0	277·0	69·2	−9·65	−69·6	0·70
31	20·0	7·36	944	0·49	35·00	115·0	36·7	67·4	178·0	259·0	30·3	−9·65	−70·5	0·72
32	19·9	8·40	920	0·58	34·90	104·0	36·2	64·4	203·0	200·0	29·6	−9·67	−66·8	0·67
33	22·0	8·25	967	1·26	36·20	118·0	36·7	17·6	289·0	246·0	1·0	−9·12	−65·3	0·75
34	19·0	7·77	924	0·68	28·20	120·0	36·5	52·2	201·0	246·0	39·3	−8·96	−66·0	0·72
35	18·9	7·50	1182	1·97	27·40	159·0	39·4	31·6	351·0	259·0	40·8	−8·87	−65·1	0·91
36	19·5	8·05	1103	1·25	20·80	98·7	39·2	15·8	396·0	256·0	3·5	−6·58	−59·8	0·83
37	23·8	8·32	1454	7·23	45·50	198·0	45·9	77·4	531·0	132·0	39·8	−6·59	−51·1	1·08
38	23·5	6·50	2206	4·04	43·20	358·0	77·4	22·6	1028·0	159·0	0·05	−9·25	−65·2	1·69
39	18·0	7·70	910	1·50	14·60	142·0	33·9	17·8	287·0	226·0	4·8	−8·48	−59·8	0·73
40	19·2	7·60	544	1·80	14·40	62·9	26·5	18·8	55·7	252·0	3·0	−8·83	−61·9	0·44
41	19·5	7·86	1148	3·00	30·80	164·0	40·5	32·5	426·0	192·0	27·6	−9·23	−62·8	0·92
42	18·5	8·00	576	1·36	8·12	80·4	21·4	13·9	95·0	271·0	21·5	−9·25	−65·4	0·51
43	18·2	7·78	1140	2·37	6·20	168·0	59·9	10·0	535·0	284·0	0·0	−9·45	−69·0	1·07
44	22·0	7·06	957	4·56	28·20	156·0	28·8	19·9	408·0	195·0	13·5	−7·60	−57·9	0·85
45	22·0	8·51	594	1·84	21·50	80·6	11·6	15·9	120·0	179·0	11·8	−9·64	−65·2	0·44
46	18·5	7·76	980	1·19	11·70	146·0	26·2	11·3	261·0	261·0	13·3	−8·65	−63·5	0·73
47	18·3	7·73	390	0·83	9·50	69·4	11·3	6·9	106·0	151·0	13·2	−9·65	−68·5	0·37

Table 2. Chemical data and in situ physico-chemical parameters of the collected samples

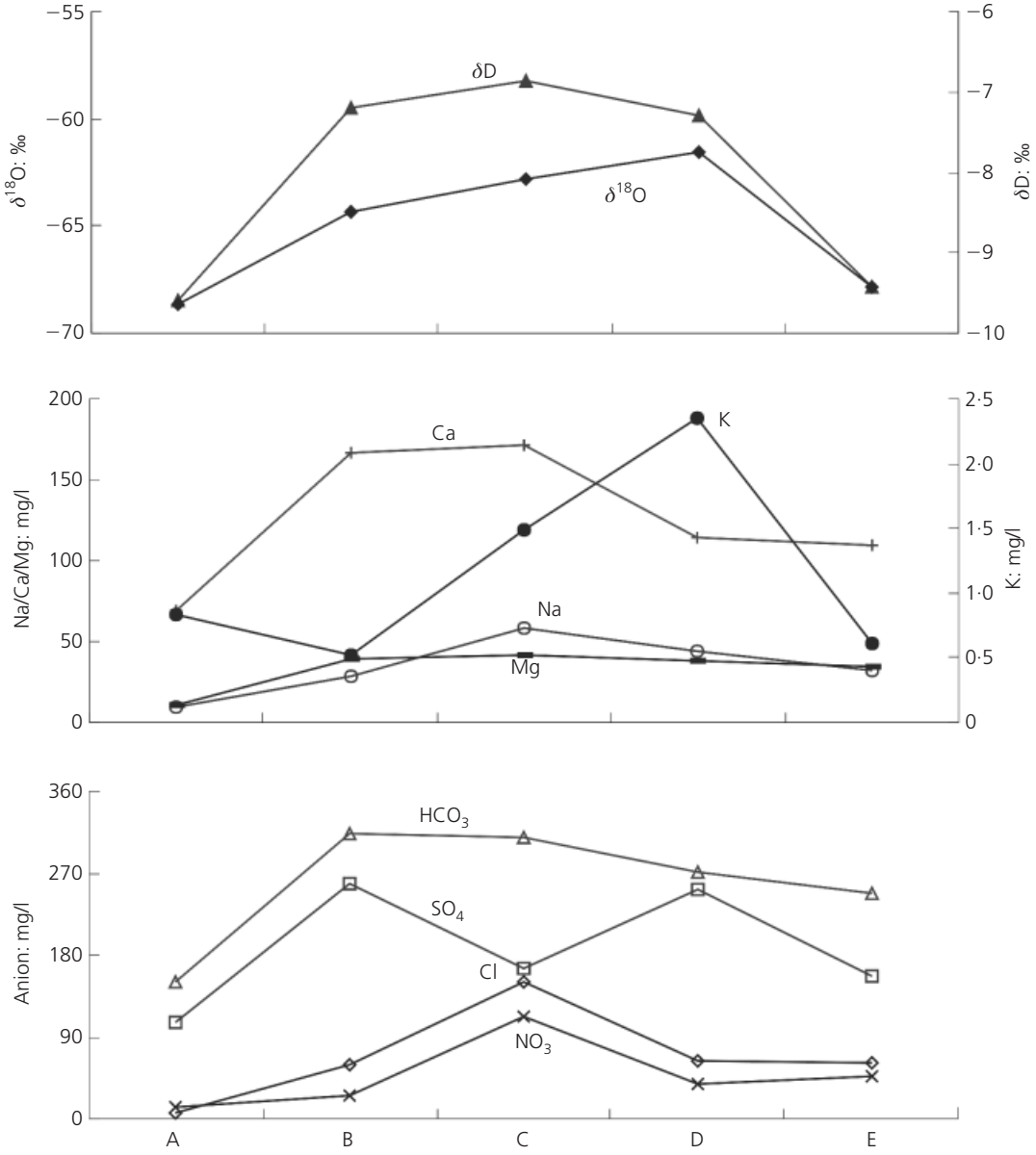

Figure 4. Variation of major ions, δ^{18}O and δD in groundwater along the flow path. A, recharge area, using the representative water sample 47. B, central coal mining area, the average value of samples 10, 12, 15 and 16. C, central industrial and densely populated residential area, the average value of samples 5, 7, 17 and 18. D, lower flow-through area, the average value of samples 28, 36 and 40. E, discharge area, the average value of the five spring water samples

parameters of the groundwater samples is shown in Table 3. A moderate to high variability of the parameters was observed among groundwater samples, as indicated by their standard deviations and coefficients of variation. The highest variability was for HCO_3^-, followed by, NO_3^-, Na^+, SO_4^{2-}, K^+ and δ^{18}O, with coefficient of variation values above 1·0, which reflects the spatial variation of groundwater quality in NKWS. According to the result of box and whisker plots of the major ions in the groundwater, Cl^- and SO_4^{2-} showed the largest variability, followed by HCO_3^-, Ca^{2+}, NO_3^- and Na^+ (Figure 5).

The hydrochemical type of groundwater in the study area varies from the HCO_3-Ca-Mg type through HCO_3-SO_4-Ca or HCO_3-Cl-Ca to the SO_4-HCO_3-Ca-Mg, Cl-SO_4-HCO_3-Ca-Mg, SO_4-Ca-Mg

	Max.	Min.	Mean	SD	CoV: %	Skewness
T: °C	20·0	15·5	18·5	1·10	5·95	−0·93
pH	8·40	7·12	7·62	0·26	3·47	0·66
EC: μS/cm	1805	390	993	404	40·7	0·51
K^+: mg/l	3·99	0·01	1·01	0·99	97·4	1·20
Na^+: mg/l	98·3	3·49	26·4	22·2	83·9	1·54
Ca^{2+}: mg/l	280	54·2	134	60·5	45·1	0·81
Mg^{2+}: mg/l	74·7	11·3	36·6	15·9	43·5	0·74
Cl^-: mg/l	244	6·13	49·4	56·2	114	1·98
SO_4^{2-}: mg/l	750	10·2	231	198	85·7	1·22
HCO_3^-: mg/l	582	145	267	87·8	32·9	2·26
NO_3^-: mg/l	149	0	38·8	37·8	97·4	1·64
$\delta^{18}O$: ‰	−6·58	−9·93	−8·76	0·81	−9·29	1·03
δD: ‰	−50·2	−70·5	−62·7	4·71	−7·50	0·59
TDS: g/l	1·47	0·35	0·78	0·32	40·5	0·58

Table 3. Descriptive statistics of chemical composition of groundwater in NKWS ($N = 32$, including spring water)

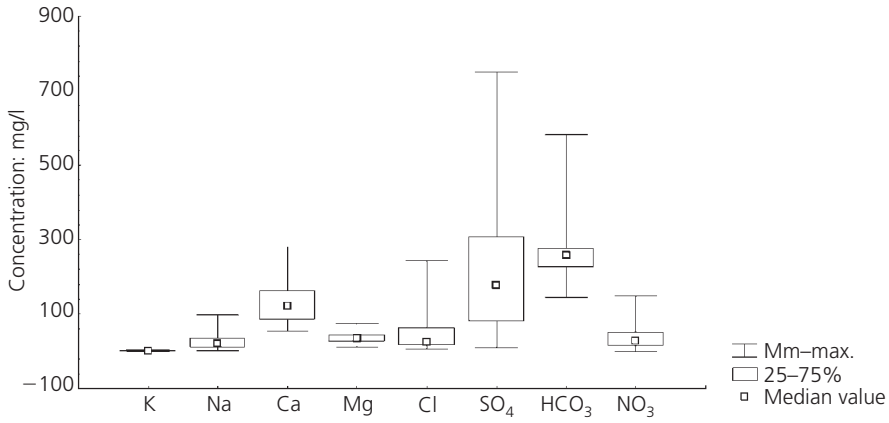

Figure 5. Box and whisker plots of major ions in karst water of the NKWS

or SO_4-Ca type as groundwater moves from the recharge area into the flow-through area or discharge areas. Generally, Ca^{2+}, Mg^{2+} and HCO_3^- were the dominant cations and anions in the groundwater samples collected from the recharge area and south/north flow-through area, with little disturbance due to human activity, suggesting that natural water–rock interaction was the primary process controlling Ca^{2+}, Mg^{2+} and HCO_3^- in the groundwater from these areas. On the other hand, relatively high concentrations of SO_4^{2-}, Cl^-, NO_3^- and Ca^{2+} were observed in samples collected from the mining area and the natural and artificial discharge areas, suggesting anthropogenic inputs of high Cl^-, NO_3^-, SO_4^{2-} and Ca^{2+} in the groundwater of these areas (Figure 3).

4.2 Assessment of human activity contribution

A total of 14 variables (groundwater temperature *T*, pH, EC, K^+, Na^+, Ca^{2+}, Mg^{2+}, Cl^-, SO_4^{2-}, HCO_3^-, NO_3^-, $\delta^{18}O$, δD and TDS) were used for factor analysis. The correlation matrix of these hydrochemical variables is given in Table 4. The Kaiser criterion method (Cooley and Lohnes, 1971) was employed to extract the maximum number of factors; this takes into account only factors having eigenvalues larger than one. In this way, three factors were obtained and rotated according to the Varimax method (Cooley and Lohnes, 1971). The marked loadings are larger than 0·7 (shown in Table 5 in bold font). These factors account for 78·5% of the total variance. The difference in the loadings of the three factors reflects the different processes and factors responsible for the chemical characteristics of groundwater in the karst water system.

Factor 1 accounts for about 46·7% of the total variance, and was chiefly composed of pH, EC, Na^+, Ca^{2+}, Mg^{2+}, SO_4^{2-} and TDS. The significantly high positive loading of Ca^{2+} and Mg^{2+}

	T: °C	pH	EC: μS/cm	K^+: mg/l	Na^+: mg/l	Ca^{2+}: mg/l	Mg^{2+}: mg/l	Cl^-: mg/l	SO_4^{2-}: mg/l	HCO_3^-: mg/l	NO_3^-: mg/l	$\delta^{18}O$: ‰	δD: ‰	TDS: g/l
T: °C	1·000	0·163	0·322*	0·743†	0·285	0·284	0·160	0·216	0·250	−0·284	0·164	0·491†	0·371*	0·262
pH	0·163	1·000	−0·741†	−0·137	−0·661†	−0·591†	−0·725†	0·194	−0·760†	0·242	0·174	0·166	0·092	−0·744†
EC: μS/cm	0·322*	−0·741†	1·000	0·588†	0·768†	0·834†	0·786†	0·125	0·888†	−0·391†	−0·011	0·226	0·252	0·897†
K^+: mg/l	0·743†	−0·137	0·588†	1·000	0·357*	0·526†	0·280	0·130	0·437†	−0·278	0·210	0·554†	0·481†	0·449†
Na^+: mg/l	0·285	−0·661†	0·768†	0·357*	1·000	0·575†	0·942†	0·072	0·912†	−0·406†	−0·033	0·147	0·195	0·925†
Ca^{2+}: mg/l	0·284	−0·591†	0·834†	0·526†	0·575†	1·000	0·708†	0·142	0·780†	−0·172	0·025	0·306*	0·319*	0·827†
Mg^{2+}: mg/l	0·160	−0·725†	0·786†	0·280	0·942†	0·708†	1·000	−0·033	0·950†	−0·301*	−0·119	0·072	0·117	0·967†
Cl^-: mg/l	0·216	0·194	0·125	0·130	0·072	0·142	−0·033	1·000	−0·083	0·031	0·587†	0·331*	0·390†	0·049
SO_4^{2-}: mg/l	0·250	−0·760†	0·888†	0·437†	0·912†	0·780†	0·950†	−0·083	1·000	−0·483†	−0·212	0·162	0·194	0·976†
HCO_3^-: mg/l	−0·284	0·242	−0·391†	−0·278	−0·406†	−0·172	−0·301*	0·031	−0·483†	1·000	0·344*	−0·185	−0·254	−0·330*
NO_3^-: mg/l	0·164	0·174	−0·011	0·210	−0·033	0·025	−0·119	0·587†	−0·212	0·344*	1·000	0·332*	0·365*	−0·053
$\delta^{18}O$: ‰	0·491†	0·166	0·226	0·554†	0·147	0·306*	0·072	0·331*	0·162	−0·185	0·332*	1·000	0·883†	0·196
δD: ‰	0·371*	0·092	0·252	0·481†	0·195	0·319*	0·117	0·390†	0·194	−0·254	0·365*	0·883†	1·000	0·229
TDS: g/l	0·262	−0·744†	0·897†	0·449†	0·925	0·827†	0·967†	0·049	0·976†	−0·330*	−0·053	0·196	0·229	1·000

* Significance at 0·05 significant level
† Significance at 0·01 significant level

Table 4. The correlation matrix of groundwater quality

Parameter	Factor 1	Factor 2	Factor 3
T	0·101	**0·797**	−0·0375
pH	**0·856**	0·235	0·129
EC	**0·895**	0·288	−0·00274
K^+	0·330	**0·772**	0·0239
Na^+	**0·889**	0·178	−0·0564
Ca^{2+}	**0·801**	0·278	0·131
Mg^{2+}	**0·950**	0·0462	−0·0710
Cl^-	0·0184	0·283	**0·732**
SO_4^{2-}	**0·949**	0·206	−0·213
HCO_3^-	−0·277	−0·460	0·560
NO_3^-	−0·0662	0·193	**0·872**
$\delta^{18}O$	0·0307	**0·837**	0·272
δD	0·0886	**0·776**	0·318
TDS	**0·974**	0·188	−0·0128
Explanatory variable	5·93	3·19	1·87
Proportion total	0·423	0·228	0·134
Eigenvalue	6·53	3·05	1·41
% of total variance	46·7	21·8	10·1
% cumulative	46·7	68·4	78·5

Table 5. Factor loadings after Varimax rotation (values in bold are those with loadings >0·7)

suggests that these variables are closely associated with water–rock interaction since Ca^{2+} and Mg^{2+} in karst groundwater arise primarily from the dissolution of carbonate (calcite and dolomite) (Aiuppa *et al.*, 2003; Eisenlohr *et al.*, 1999; Leybourne *et al.*, 2009; Moore *et al.*, 2009). However, the indistinctive correlations between Ca^{2+}, Mg^{2+}, TDS and HCO_3^- (Table 4) suggest that in the NKWS area, water–rock interaction is not the only (and perhaps not even the major) reason for the high loading of these ions. Water with high factor 1 scores was in all cases found in the samples with high SO_4^{2-} content. Sources of SO_4^{2-} include rainfall (Williams and Melack, 1991), fertilisers (Hosono *et al.*, 2007; Knights *et al.*, 2000; Valdes *et al.*, 2007), sewage effluent (Oren *et al.*, 2004), and dissolution of sulphide minerals (Szynkiewicz *et al.*, 2009) and sulphate (gypsum). As discussed later, dissolution of gypsum constitutes one source for sulphate in groundwater from the NKWS. However, the average SO_4^{2-} content of 231 mg/l implies that there might be additional sources of sulphate.

As one of the largest coal mining areas in northern China, the impacts of coal mining may play an important role in determining groundwater chemistry in the study area. In other words, the high positive loadings of Ca^{2+}, Mg^{2+} and SO_4^{2-} may be due primarily to coal mining. The high positive loadings of EC and TDS, and the strong negative loading of pH, support this interpretation. Elevated EC and TDS are consistent with coal mining activity, not only because of the solutes in the mining wastewater, but also because the acidic character of the mine drainage may accelerate the dissolution of aquifer materials such as calcite, dolomite and gypsum. In addition, the relatively negative correlation between pH and SO_4^{2-} suggests that there should be additional sources of sulphate, such as coal mining.

According to previous work using sulphate–sulphur isotope (Li and Wang, 2003), coal mining activity has a strong impact on sulphate content increase at the NKWS. A more detailed hydrogeochemical analysis can provide important clues about the sources of calcium, magnesium and sulphate in karst groundwater (Wang *et al.*, 2006). Assuming that all the calcium and magnesium is from calcite, dolomite and gypsum and that all the sulphate in the groundwater is from gypsum dissolution in the study area, the quantity of calcium from dissolution of calcite and dolomite can be calculated by subtracting the amount of calcium from gypsum dissolution from total calcium, expressed as $[Ca^{2+}]-[SO_4^{2-}]$ in mmol/l concentration, and the concentration of calcium derived from gypsum dissolution can be characterised as $[Ca^{2+}]-0{\cdot}33[HCO_3^-]$, according to the stoichiometry of the dissolution reactions of calcite and dolomite (Wang *et al.*, 2006). Therefore, a 1:4 relationship line suggests the congruent dissolution of dolomite, a 1:2 relationship line suggests dissolution of calcite in the bicarbonate plotted against $[Ca^{2+}]-[SO_4^{2-}]$ (calcium obtained from non-sulphate minerals) plot, and groundwater samples located between the 1:4 and the 1:2 relationship lines suggest congruent dissolution of calcite and dolomite. About half of the samples from the NKWS are plotted around the 1:4 relationship line, indicating a greater contribution from dolomite dissolution to calcium and bicarbonate concentrations in these karst waters (Figure 6). Furthermore, some of the water samples fall below the $[Ca^{2+}]-[SO_4^{2-}] = 0$ line, indicating the effect of surplus sulphate in the water samples. The contribution of congruent gypsum dissolution to sulphate concentration can be clearly seen from a 1:1 linear molarity relationship between non-carbonate calcium and sulphate (Figure 7). Although about half of the karst water samples are scattered around the 1:1 non-carbonate source calcium and sulphate relationship line,

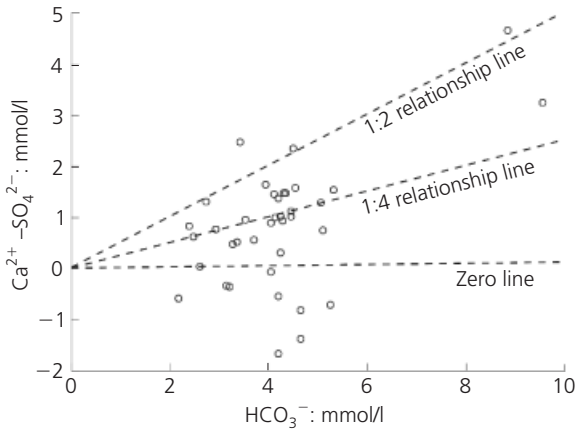

Figure 6. Bicarbonate concentration plotted against non-gypsum source calcium concentration in karst water

samples with sulphate content higher than 3 mmol/l are shifted to the right away from the 1:1 relationship line, indicating again additional inputs of sulphate, such as oxidation of sulphide minerals in the Carboniferous–Permian coal-bearing strata during coal mining activities (Li and Wang, 2003) and discharge of municipal sewage into surface waters that then leak into the groundwater system along river channels.

Karst water samples plotted around the 1:4 relationship line in Figure 8 suggest congruent dissolution of dolomite, according to the stoichiometry of the dissolution reaction of dolomite. However, most of the samples fall above the line due to elevated magnesium concentrations in addition to CO_2 dissolution of dolomite. Under the impact of anthropogenic inputs of sulphate in the karst water, dolomite dissolution and calcite precipitation (dedolomitisation) may be enhanced due to the common-ion effect, as suggested by the relatively invariable bicarbonate concentration and elevated magnesium concentration in Figure 8. It is interesting to see that there are two trend lines in the plot of Mg^{2+} against SO_4^{2-} (Figure 9), with a dramatic increase of magnesium content with sulphate content higher than 5 mmol/l,

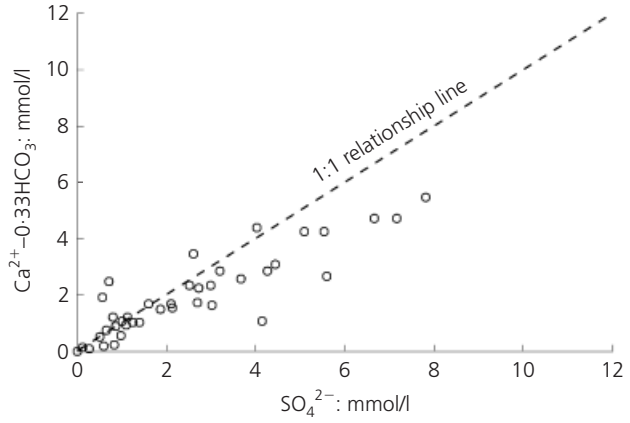

Figure 7. Sulphate concentration plotted against non-carbonate calcium concentration in karst water

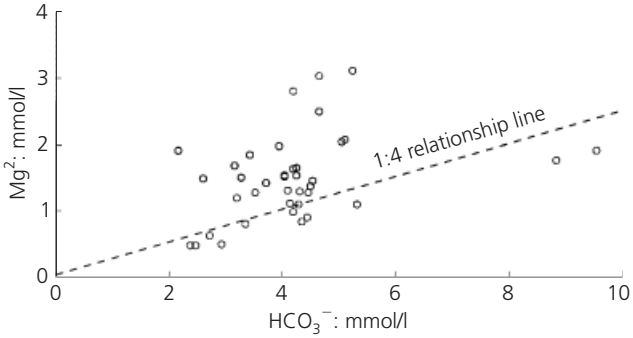

Figure 8. Bicarbonate concentration plotted against magnesium concentration in karst water

indicating the effect of anthropogenic sulphate on intensification of the dedolomitisation process.

Inputs of Na^+ to groundwater arise primarily from the incongruent dissolution of plagioclase, the dissolution of chemical fertilisers, the disposal of domestic effluent and atmospheric input through the infiltration of precipitation (Bhatt and McDowell, 2007; Kass *et al.*, 2005; Neal and Kirchner, 2000). The content of sodium in precipitation is as low as 0·03–0·2 mmol/l in the study area. And, since the major karst aquifers at the NKWS are composed of carbonate rocks, water–plagioclase interaction may not be a major source for sodium in the groundwater. Therefore, the elevated contents of sodium in groundwater should be linked with human activities.

To sum up, factor 1 is more indicative of the effect of human activity (primarily coal mining) than that of water–rock interaction.

Factor 2, accounting for about 22% of the total variance, consists of T (groundwater temperature), K^+, $\delta^{18}O$ and δD. The significantly high positive loadings of T, $\delta^{18}O$ and δD suggest that those variables are associated primarily with recharge from surface water. As mentioned in the previous section, the $\delta^{18}O$ and δD values of surface water at Niangziguan are commonly higher than those of the groundwater because of the isotope fractionation effect by evaporation. Therefore, if groundwater from the recharged area is affected by surface water when it enters the flow-through area or the discharge area, its $\delta^{18}O$ and δD values could increase. The elevation in isotopic composition normally depends on the mixing rate and isotope characteristics of surface water. Most of the surface water samples are located on the right side of the local meteoric water line of China, reflecting the strong effect of evaporation (Figure 10), while some groundwater samples are close to surface water samples, indicating the significant recharge of surface water on them.

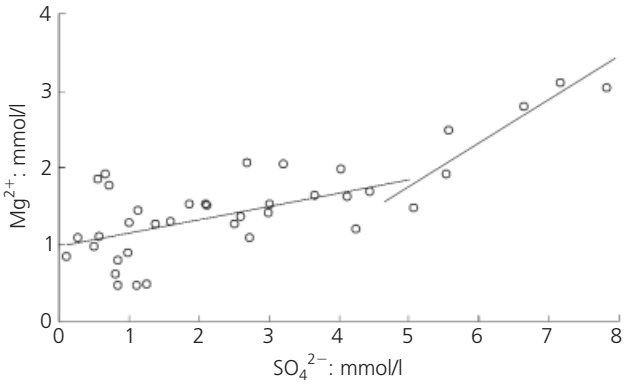

Figure 9. Sulphate concentration plotted against magnesium concentration in karst water (solid line shows the trend line of magnesium)

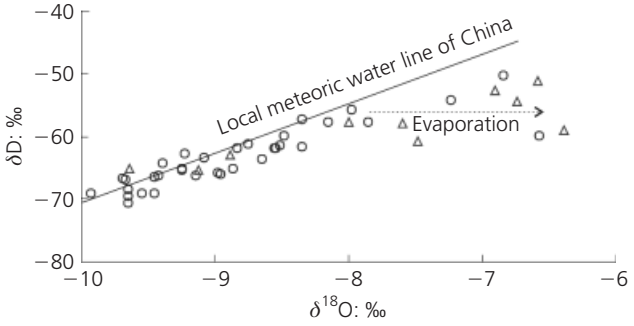

Figure 10. $\delta^{18}O$ plotted against δD plot of water samples in the study area: ○, groundwater; △, surface water

Groundwater samples with elevated temperatures are also associated with surface water.

Potassium in groundwater often comes from orthoclase and muscovite minerals present in granite, and from pollution sources such as chemical fertilisers, mining wastewater and domestic effluent (Griffioen, 2001; Watmough *et al.*, 2005). The content of K^+ in natural surface water underlain by limestone and dolomite is normally very low. In the study area, however, elevated K^+ contents were observed in most samples of the surface water located in flow-through areas where human activities are strong. So, factor 2 is interpreted to indicate the impact of human activities on surface water and consequent impact on groundwater through the process of groundwater recharge from surface water.

Factor 3, accounting for about 10% of the total variance, consists of Cl^- and NO_3^-. The significantly high positive loadings of Cl^- and NO_3^- indicate that those variables are associated with human activities. Generally, atmospheric deposition is not considered to be a major source of NO_3^- concentrations in groundwater, and the hypothesis of a geogenic source of NO_3^- would be totally inconsistent with the geologic character of the study area. Therefore, the substantial contribution of NO_3^- to groundwater in the study area likely results from excessive application of agricultural fertilisers and from seepage of sewage effluent into the subsurface.

Natural sources of Cl^- in groundwater include rainfall, the dissolution of fluid inclusions and Cl^- bearing minerals (Neal and Kirchner, 2000; Negrel and Roy, 1998) or the displacement of saline connate water into fresh water aquifers. Chloride can also derive from pollution by industrial wastes, septic systems or other sources of domestic effluent, and from the overuse of fertilisers (Edmunds *et al.*, 2003; Hosono *et al.*, 2007; Knights *et al.*, 2000; Valdes *et al.*, 2007; Widory *et al.*, 2004). There is little variation in lithology in the major aquifers in the study area, and it is clear that groundwater in the areas of greatest natural recharge is consistently low in Cl^- content. This indicates that natural sources are not primarily responsible for the Cl^- content of the groundwater. Thus, the high Cl^- content in the groundwater could be related to human activities. The highest Cl^- contents are typically found in (or downgradient of) areas with strong human activities such as mining areas, industrial areas and densely populated residential areas (Figure 3). Human activities are thus largely responsible for the observed Cl^- concentrations.

4.3 Distribution of groundwater with different factor scores

Cluster analysis was performed on the factor scores of each sampling site to illustrate how clusters are distributed. The results of this analysis indicate that the water samples can be grouped into four clusters (Figure 11, Table 6). Cluster 1, which includes groundwater samples 1, 16, 19 and 43 (Table 1), is characterised by the highest factor 1 scores, the lowest factor 2 scores and medium factor 3 scores. All of these samples were near or within the mining areas in the western part of the study area (Figure 3). The high factor 1 score in these samples indicates that coal mining activities have a significant impact on the groundwater chemistry. Impacts of other kinds of human activities were also indicated, as suggested by the medium factor 3 scores. These pollutants may originate from the inorganic and organic materials in coal byproducts, the use of nitro-explosives and from sewer wastes.

The highest scores for factor 2 were found in cluster 2, which displayed the highest factor 3 scores and medium factor 1 scores (Figure 11). This cluster includes samples 5, 7, 17 and 18, which are all located in or near suburban areas of Yangquan city and close to rivers. In the vicinity of groundwater samples 5 and 7, surface water flows in channels with carbonate rocks free of overlying sediments, and the Nanchuan River water can leak and recharge the underlying karst aquifer. Although the carbonate rock is covered by 1–20 m of Quaternary sediment in the vicinity of groundwater samples 17 and 18, significant recharge of surface water in this area is also indicated by the high factor 2 scores. At the same time, the high factor 3 scores of cluster 2 show that pollution from human activities also contributes significantly to the groundwater chemistry of this cluster.

The highest factor 3 scores were found in cluster 3, which includes the largest number of groundwater samples (samples 10,

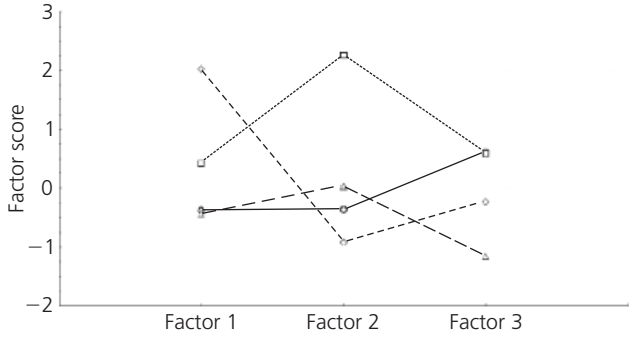

Figure 11. Average factor scores for each cluster: ◇, cluster 1; □, cluster 2; ○, cluster 3; △, cluster 4

		Cluster 1	Cluster 2	Cluster 3	Cluster 4
Factor 1	pH	7·53	7·52	7·75	7·51
	EC: μS/cm	1665	1452	922	806
	Na^+: mg/l	27·1	64·0	17·6	12·2
	Ca^{2+}: mg/l	251	168	112	99·7
	Mg^{2+}: mg/l	70·1	43·4	31·6	30·8
	$SO_4{}^2$: mg/l^-	663	111	222	88·3
Factor 2	*T*: °C	18·4	19·3	18·7	18·2
	K^+: mg/l	1·12	1·60	1·01	0·090
	$\delta^{18}O$: ‰	−9·11	−8·25	−8·79	−9·50
	δD: ‰	−63·0	−58·6	−62·4	−66·6
Factor 3	Cl^-: mg/l	26·4	148	18·6	19·5
	$HCO_3{}^-$: mg/l	284	245	249	269
	$NO_3{}^-$: mg/l	12·0	114	28·6	28·4

Table 6. Median values for clusters, arranged according to principal components model

12, 13, 21, 28, 32, 34–36, 40–42, 46 and 47). These samples were mostly from the flow-through area and the discharge area, both with high population density. In contrast to cluster 2, the low factor 2 scores of cluster 3 indicate that there is no significant impact of surface water in cluster 3. Therefore, the significant impact of human activity may be caused by direct infiltration of local sewage waste, fertiliser and industrial waste, at concentrations little changed from surface environmental conditions. In general, the results of the cluster analysis confirm that groundwater quality in the flow-through area and discharge area has been seriously affected by human activities.

Cluster 4 (including groundwater samples 2–4, 5, 24, 26, 27 and 29–31) displays the lowest factor 1 and factor 3 scores and a medium factor 2 score. This indicates that groundwater in this cluster has been little affected by human activities and that a slight impact of surface water inflow exists. Most of the samples in this cluster were taken in the recharge area, except for the three spring waters and sample 15 from the flow-through area. The results for this cluster can thus be regarded as representatives of the background groundwater chemistry of the study area. Because of the thin cover of unconsolidated sediment and a widespread exposed carbonate rock area, recharge from surface into groundwater is still inevitable in the study area, even in the recharge area. The groundwater in most regions of the study area is affected by human activities, except for the recharge area, as indicated by the factor 3 scores: those of clusters 1, 2 and 3 are all higher than that of cluster 4 (the background value). The negative impact of coal mining was indicated primarily by the higher factor 1 scores in clusters 2 and 1 compared with that of the background value (cluster 4). In dry seasons, most of the rivers in the study area are dry, and mining and municipal wastewaters maintain the river flow. Owing to recharge from polluted rivers, degradation of groundwater quality in these areas is inevitable.

5. Conclusions

The chemical characteristics of groundwater in the NKWS were investigated to understand the degree to which human activities affect groundwater quality. The study results show that human activities have a significant impact on the chemical composition of groundwater.

The hydrochemical types change from HCO_3-Ca-Mg or HCO_3-SO_4-Ca-Mg type to SO_4-HCO_3-Ca, Cl-SO_4-HCO_3-Ca, SO_4-Ca and SO_4-Cl-Ca type because of increases in $SO_4{}^{2-}$, Cl^- and $NO_3{}^-$ concentrations. Results from factor analysis indicate that abnormally high $SO_4{}^{2-}$ and Na^+ were mainly from sources related to coal mining activities, which are widely distributed in the study area. Potassium was mainly from sources related to recharge by contaminated surface water. Chloride and nitrate were primarily from human-related activities such as agriculture, wastewater discharge and sewage effluent release. The results of cluster analyses using the factor scores indicate that natural processes and different kinds of human activity have been the major controlling factors in determining the groundwater chemistry. The results of this study also provide some clues about the sources of groundwater contamination in the NKWS. This work demonstrates that multi-variate analysis, coupled with hydrogeochemical analysis, is a useful tool to characterise the potential impact of human activities on groundwater quality.

Acknowledgements

This research work was financially supported by the National Natural Science Foundation of China (no. 40830748), the Minis-

try of Education of China (111 project) and China Geological Survey (no. CGS-200310400009).

REFERENCES

Aiuppa A, Bellomoa S, Bruscab L, Alessandrob WD and Federico C (2003) Natural and anthropogenic factors affecting groundwater quality of an active volcano (Mt. Etna, Italy). *Applied Geochemistry* **18(6)**: 863–882.

Aravena R, Auge M, Bucich N and Nagy MI (1999) Evaluation of the origin of groundwater nitrate in the city of La Plata, Argentina, using isotope techniques. *Proceedings of XXIX IAH Congress on Hydrogeology and Land Use Management, Bratislava*, 6–10.

Bakalowicz M (2005) Karst groundwater: a challenge for new resources. *Hydrogeology Journal* **13(1)**: 148–160.

Baker T and Groves C (2008) Water quality impacts from agricultural land use in karst drainage basins of SW Kentucky and SW China. *Proceedings of 3rd Interagency Conference on Research in the Watersheds, Estes Park, CO*, 8–11.

Bhatt MP and McDowell WH (2007) Controls on major solutes within the drainage network of a rapidly weathering tropical watershed. *Water Resources Research* **43(11)**: W11402.1–W11402.9.

Bonacci O, Gottstein S and Roje-Bonacci T (2009) Negative impacts of grouting on the underground karst environment. *Ecohydrology* **2(4)**: 492–502.

Cooley WW and Lohnes PR (1971) *Multivariate Data Analysis*. Wiley, New York.

Denimal S, Tribovillard N, Barbecot F and Dever L (2002) Leaching of coal-mine tips (Nord-Pas-de-Calais coal basin, France) and sulphate transfer to the chalk aquifer: example of acid mine drainage in a buffered environment. *Environmental Geology* **42(8)**: 966–981.

Edmunds WM, Shand P, Hart P and Ward RS (2003) The natural (baseline) quality of groundwater: a UK pilot study. *Science of the Total Environment* **310(1–3)**: 25–35.

Eisenlohr L, Meteva K, Gabrovsek F and Dreybrodt W (1999) The inhibiting action of intrinsic impurities in natural calcium carbonate minerals to their dissolution kinetics in aqueous H_2O–CO_2 solutions. *Geochimica et Cosmochimica Acta* **63(7–8)**: 989–1001.

Epstein S and Mayeda TK (1953) Variations of the $^{18}O/^{16}O$ ratio in natural waters. *Geochimica et Cosmochimica Acta* **4**: 213–224.

Farnham IM, Stetzenbach KJ, Singh AK and Johannesson KH (2000) Deciphering groundwater flow systems in Oasis Valley, Nevada, using trace element chemistry, multivariate statistics, and geographical information system. *Mathematical Geology* **32(8)**: 943–968.

Ford DC and Williams PW (2007) *Karst Hydrogeology and Geomorphology*. Wiley, Chichester.

Gao XB, Wang YX, Li YL and Guo QH (2007) Enrichment of fluoride in groundwater under the impact of saline water intrusion at the salt lake area of Yuncheng basin, northern China. *Environmental Geology* **53(4)**: 795–803.

Gao XB, Wang YX, Wu PL and Guo QH (2010) Trace elements and environmental isotopes as tracers of surface water-groundwater interaction: A case study at Xin'an karst water system, Shanxi Province, Northern China. *Earth and Environmental Science* **59(6)**: 1223–1234.

Ghiglieri G, Barbieri G, Vernier A *et al.* (2009) Potential risks of nitrate pollution in aquifers from agricultural practices in the Nurra region, northwestern Sardinia, Italy. *Journal of Hydrology* **379(3–4)**: 339–350.

Glassmeyer ST, Furlong ET, Kolpin DW, *et al.* (2005) Transport of chemical and microbial compounds from known wastewater discharges: potential for use as indicators of human fecal contamination. *Environmental Science and Technology* **39(14)**: 5157–5169.

Glynn PD and Plummer LN (2005) Geochemistry and the understanding of ground-water systems. *Hydrogeology Journal* **13(1)**: 263–287.

Griffioen J (2001) Potassium adsorption ratios as an indicator for the fate of agricultural potassium in groundwater. *Journal of Hydrology* **254(1–4)**: 244–254.

Hao YH, Wang YJ, Zhu Y, *et al.* (2009) Response of karst springs to climate change and anthropogenic activities: The Niangziguan Springs, China. *Progress in Physical Geography* **33(5)**: 634–649.

Hatano R, Shinano T, Zheng TG, Okubo M and Li ZW (2002) Nitrogen budgets and environmental capacity in farm systems in a large-scale karst region, southern China. *Nutrient Cycling in Agroecosystems* **63(2–3)**: 139–149.

Helena B, Pardo R, Vega M, *et al.* (2000) Temporal evolution of groundwater composition in an alluvial aquifer (Pisuerga River, Spain) by principal component analysis. *Water Research* **34(3)**: 807–816.

Hosono T, Nakano T, Igeta A, *et al.* (2007) Impact of fertilizer on a small watershed of Lake Biwa: use of sulfur and strontium isotopes in environmental diagnosis. *Science of the Total Environment* **384(1–3)**: 342–354.

Jackson RB, Carpenter SR, Dahm CN, *et al.* (2001) Water in a changing world. *Ecological Applications* **11(4)**: 1027–1045.

Jiang YJ, Wu YX and Yuan DX (2009) Human impacts on karst groundwater contamination deduced by coupled nitrogen with strontium isotopes in the Nandong underground river system in Yunan, China. *Environmental Science and Technology* **43(20)**: 7676–7683.

Kass A, Gavrieli I, Yechieli Y, Vengosh A and Starinsky A (2005) The impact of freshwater and wastewater irrigation on the chemistry of shallow groundwater: a case study from the Israeli Coastal Aquifer. *Journal of Hydrology* **300(1–4)**: 314–331.

Knights JS, Zhao FJ, Spiro B and McGrath SP (2000) Long-term effects of land use and fertilizer treatments on sulfur cycling. *Journal of Environmental Quality* **29(6)**: 1867–1874.

LeGrand HE (1984) Environmental problems in karst terrains. *Hydrogeology of Karstic Terrains: Case Histories* (Burger A

and Dubertret L (eds)). UNESCO-IAH, Hanover, pp. 189–194.

Leybourne MI, Betcher RN, McRitchie WD, Kaszycki CA and Boyle DR (2009) Geochemistry and stable isotopic composition of tufa waters and precipitates from the Interlake Region, Manitoba, Canada: constraints on groundwater origin, calcitization, and tufa formation. *Chemical Geology* **260(3–4)**: 221–233.

Li YL and Wang YX (2003) Temporal–spatial variation of isotopic compositions as indicators of hydrodynamic conditions of a large karst water system. *Proceedings of International Symposium on Water Resources and the Urban Environment*, Wuhan, pp. 92–97.

Moncaster S, Bottrell SH, Tellam JH, Lloyd JW and Konhauser KO (2000) Migration and attenuation of agrochemical pollutants: insights from isotopic analysis of groundwater sulphate. *Journal of Contaminant Hydrology* **43(2)**: 147–163.

Moore PJ, Martin JB and Screaton EJ (2009) Geochemical and statistical evidence of recharge, mixing, and controls on spring discharge in an eogenetic karst aquifer. *Journal of Hydrology* **376(3–4)**: 443–455.

Neal C and Kirchner JW (2000) Sodium and chloride levels in rainfall, mist, streamwater and groundwater at the Plynlimon catchments, mid-Wales: inferences on hydrological and chemical controls. *Hydrology and Earth System Sciences* **4(2)**: 295–310.

Negrel P and Roy S (1998) Rain chemistry in the Massif Central (France): a strontium isotopic and major elements study. *Applied Geochemistry* **13(8)**: 941–952.

Oren O, Yechieli Y, Bohlke JK and Dody A (2004) Contamination of groundwater under cultivated fields in an arid environment, central Arava Valley, Israel. *Journal of Hydrology* **290(3–4)**: 312–328.

Reghunath R, Murthy TRS and Raghavan BR (2002) The utility of multivariate statistical techniques in hydrogeochemical studies: an example from Karnataka, India. *Water Research* **36(10)**: 2437–2442.

Silliman SE, Boukari M, Crane P, Azonsi F and Neal CR (2007) Observations on elemental concentrations of groundwater in central Benin. *Journal of Hydrology* **335(3–4)**: 374–388.

Spalding RF and Exner ME (1993) Occurrence of nitrate in groundwater – a review. *Journal of Environmental Quality* **22(3)**: 392–402.

Szynkiewicz A, Moore CH, Glamoclija M and Pratt LM (2009) Sulfur isotope signatures in gypsiferous sediments of the Estancia and Tularosa Basins as indicators of sulfate sources, hydrological processes, and microbial activity. *Geochimica et Cosmochimica Acta* **73(20)**: 6162–6186.

Thyne G, Guler C and Poeter E (2004) Sequential analysis of hydrochemical data for watershed characterization. *Ground Water* **42(5)**: 711–723.

Valdes D, Dupont JP, Laignel B, Ogier S, Leboulanger T and Mahler BJ (2007) A spatial analysis of structural controls on Karst groundwater geochemistry at a regional scale. *Journal of Hydrology* **340(1–4)**: 244–255.

Wang YX and Gao XB (2009) Geochemical evolution of the Niangziguan karst water system under the impact of human activities. *Carsologica Sinica* **28(2)**: 10–19 (in Chinese with English abstract).

Wang YX, Ma T and Luo ZH (2001) Geostatistical and geochemical analysis of surface water leakage into groundwater on a regional scale: a case study in the Liulin karst system, northwestern China. *Journal of Hydrology* **246(1–4)**: 223–234.

Wang YX, Guo QH, Su CL and Ma T (2006) Strontium isotope characterization and major ion geochemistry of karst water flow, Shentou, northern China. *Journal of Hydrology* **328(3–4)**: 592–603.

Watmough SA, Aherne J, Alewell C, *et al.* (2005) Sulphate, nitrogen and base cation budgets at 21 forested catchments in Canada, the United States and Europe. *Environmental Monitoring and Assessment* **109(1–3)**: 1–36.

Widory D, Kloppmann W, Chery L, *et al.* (2004) Nitrate in groundwater: an isotopic multi-tracer approach. *Journal of Contaminant Hydrology* **72(1–4)**: 165–188.

Williams MW and Melack JM (1991) Precipitation chemistry in and ionic loading to an alpine basin, Sierra-Nevada. *Water Resources Research* **27(7)**: 1563–1574.

Williams GM, Pickup RW, Thornton SF, *et al.* (2001) Biogeochemical characterisation of a coal tar distillate plume. *Journal of Contaminant Hydrology* **53(3–4)**: 175–197.

Yuan DX (1997) Sensitivity of karst process to environmental change along the Pep II transect. *Quaternary International* **37**: 105–113.

Zhang WL, Tian ZX, Zhang N and Li XQ (1996) Nitrate pollution of groundwater in northern China. *Agriculture Ecosystems and Environment* **59(3)**: 223–231.